Phys. Status Solidi C **10**, No. 5, 812–815 (2013) / **DOI** 10.1002/pssc.201200583

physica status solidi c
www.pss-c.com
current topics in solid state physics

Carrier lifetimes in green emitting InGaN/GaN disks-in-nanowire and characteristics of green light emitting diodes

Shafat Jahangir*, **Animesh Banerjee, and Pallab Bhattacharya**

Center for Photonics and Multiscale Nanomaterials, Department of Electrical Engineering and Computer Science, University of Michigan, Ann Arbor, MI 48109-2122, USA

Received 17 August 2012, revised 20 November 2012, accepted 27 November 2012
Published online 1 February 2013

Keywords quantum efficiency, carrier lifetime, surface passivation, disks-in-nanowire

* Corresponding author: e-mail shafat@umich.edu

Improvement in the internal quantum efficiency (IQE) of InGaN/GaN disks-in-nanowires by surface passivation is demonstrated. The highest IQE achieved through surface passivation for green emitting (λ=540 nm) InGaN/GaN disks-in-nanowires is ~53%. Radiative and nonradiative carrier lifetimes are calculated for as-grown and surface passivated green emitting disks-in-nanowires. Passivated green sample exhibits a room temperature radiative lifetime of ~748 ps, which is much smaller than that of equivalent quantum wells. Electroluminescence measurements on passivated green light emitting diodes containing InGaN disks demonstrate no roll over or efficiency droop up to 375 A/cm^2, and exhibit a blue-shift of 7 nm in peak wavelength. An enhancement in the light output due to surface passivation is observable in the relative external quantum efficiency of the surface passivated devices as compared with the as-grown samples.

© 2013 WILEY-VCH Verlag GmbH & Co. KGaA, Weinheim

1 Introduction III-N nanowires grown on silicon and the quantum-confined heterostructures contained therein are attractive for the development of visible LEDs [1-4]. The nanowires are relatively strain- and defect-free, as compared with quantum wells grown on c-plane sapphire. However, the radiative and non-radiative lifetimes in these heterostructures are largely unknown. We have performed temperature dependent photoluminescence (TDPL) and time-resolved PL (TRPL) measurements on green emitting (λ=540 nm) InGaN/GaN quantum disks in nanowires and have studied the effects of surface passivation on the radiative and non-radiative lifetimes and quantum efficiency. We have also fabricated and characterized LEDs with as-grown and surface passivated green emitting InGaN/GaN disks-in-nanowires to investigate the roll of passivation on light output.

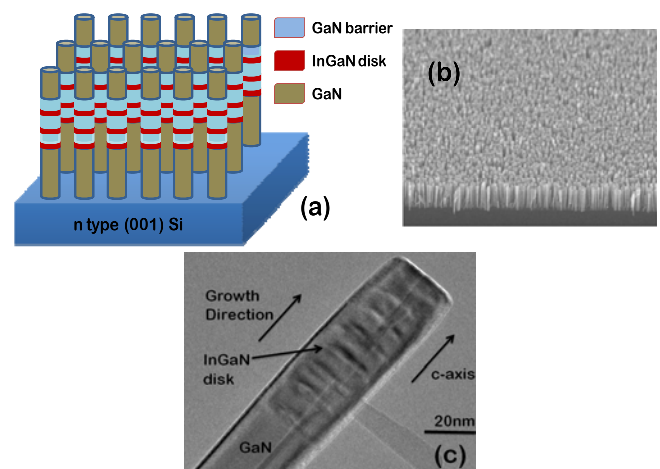

Figure 1 (a) Schematic of InGaN/ GaN disks-in- nanowires, (b) 45 degree tilted SEM image showing the morphology of the nanowires grown on a (001) Si substrate, (c) TEM image of a GaN nanowire with multiple InGaN disks.

2 Growth of samples Green emitting (λ=540nm) InGaN/GaN disks-in-nanowires (NW), shown schematically in Fig. 1(a), were grown on (001) Si substrates in a Veeco Gen II plasma-assisted molecular beam epitaxy (PA-MBE) system. Before epitaxy, the native oxide was removed from the substrate surface by rinsing the substrates in a buffered HF solution and then heating them in the growth chamber at 950 °C for 1 hr. The substrate tem-

WILEY ONLINE LIBRARY

© 2013 WILEY-VCH Verlag GmbH & Co. KGaA, Weinheim

perature was then lowered to 800 °C and a few monolayers of Ga were deposited with a Ga flux of 8 × 10^{-8} Torr in the absence of N. GaN nanowires were then grown at 800 °C at a rate of 300 nm/h under N-rich conditions with Ga flux maintained at 8 × 10^{-8} Torr and the N flow rate held constant at 1 sccm. After growing 300 nm of seed GaN

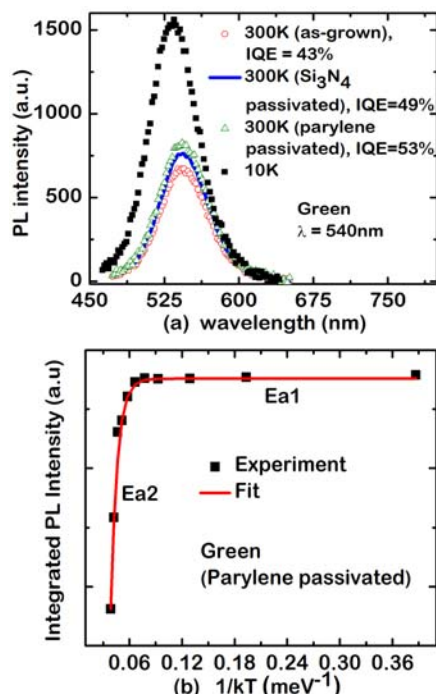

Figure 2 (a) TDPL of as-grown and surface passivated green emitting InGaN/ GaN disks-in- nanowires, (b) Arrhenius plot to calculate activation energy.

nanowire, the substrate temperature was lowered to 532 °C to grow ~2 nm thick InGaN disks, separated by 12 nm thick GaN barriers. Fig. 1(b) depicts a cross-sectional scanning electron microscopy (SEM) image of the nanowires, which have an areal density of ~2x10^{11} cm^{-2}, and average diameter of ~60 nm. A single nanowire with the InGaN disks is shown in the transmission electron microscopy (TEM) image of Fig. 1(c). Light-emitting diodes (LEDs) [shown schematically in Fig. 4] were fabricated with an epitaxially grown p-i-n structure with InGaN/GaN green emitting disk-in-NWs on n-type (001) Si. Three hundred nanometer of Si-doped n-type GaN nanowire is first grown, followed by 8 pairs of InGaN(2nm)/GaN(12nm) disks as the active region, 15nm p-$Al_{0.15}Ga_{0.85}N$ electron blocking layer (EBL) and a 150 nm Mg-doped p-type GaN on top. The nanowires were planarized with a parylene-insulating layer. Ni/Au (5 nm/5 nm) and indium tin oxide (ITO) (200 nm) were deposited as the top ohmic contact to the p-GaN nanowires. Aluminum was deposited on the n-type Si to form the bottom electrode. Measured IQE of parylene passivated InGaN/GaN disks-in-NW, used in LEDs, was ~33%. To examine the effect of surface passivation on light output, multiple devices of two different types (sample A and sample B) have been fabricated. In sample A, the nanowires are surface passivated with parylene, where sample B is unpassivated.

3 Results and discussion

3.1 Internal quantum efficiency

Temperature dependent photoluminescence (TDPL) measurements were performed on as-grown and surface passivated disks-in-

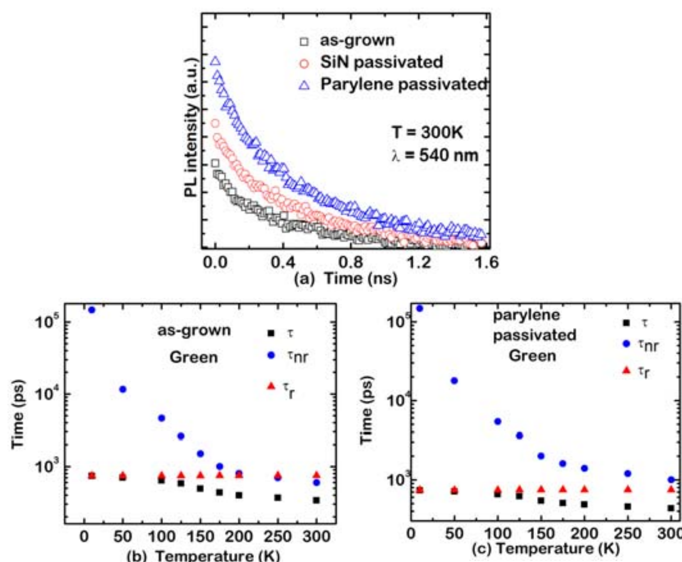

Figure 3 (a) Room temperature PL decay times, obtained from TRPL, for green emitting as-grown, Si_3N_4 passivated, and parylene passivated samples. Trend in carrier lifetimes with temperature for (b) as-grown and (c) parylene passivated samples.

NW samples to measure the internal quantum efficiency (IQE). The InGaN disks were selectively excited with a laser at λ=405 nm. The peak photoluminescence (PL) intensities at 300 K and 10 K increase with optical excitation. They reach their maximum values at different excitations, where the electron-hole wave-function overlap reaches a maximum due to complete screening of the polarization field in the disks. The peak intensity remains fairly constant with further increase in optical excitation. The value

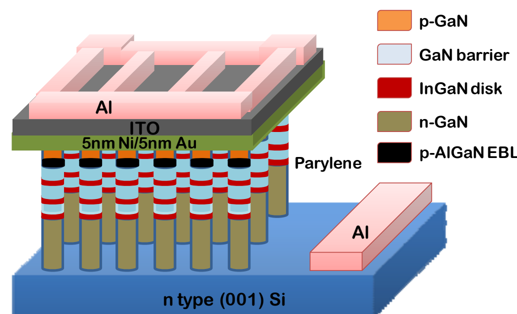

Figure 4 Schematic of InGaN/GaN disks-in-nanowires light emitting diode.

© 2013 WILEY-VCH Verlag GmbH & Co. KGaA, Weinheim

of IQE was obtained as the ratio of PL intensity at 300 K to that at 10 K at an optical excitation where both the PL intensities are at their maximum values, assuming nonradiative centers are frozen at 10 K. We measured a maximum IQE of ~53% for the parylene passivated disks, whereas it was 43% and 49% for as-grown and Si_3N_4 passivated samples, respectively. As seen in Fig. 2(a), peak wavelength shows a blueshift at low temperature in accordance with the Varshni relation [5]. Due to the large surface-to-volume ratio and the presence of surface states, nonradiative carrier recombination through these surface states can be significant in the nanowires [6]. It has also been shown that the presence of band bending on the lateral surfaces of nanowires, due to space-charge related surface depletion [7,8], can lead to further enhancement of surface recombination [9]. With passivation, the surface state density and the extent of the depletion region is reduced [10], thereby decreasing the nonradiative surface recombination rate and increasing the IQE. Parylene contributed to a slightly better surface passivation compared to Si_3N_4, increasing the IQE of the as-grown samples by ~10%.

From the fitting of Arrhenius plot, derived from TDPL measurements, two activation energies (E_{a1} =58 meV and E_{a2} =1.34 eV) are obtained [Fig. 2(b)]. The origins of these activation energies still need to be investigated. The photoluminescence intensity decreases as the temperature increases, indicating carriers recombine more non-radiatively through defects present in the system.

3.2 Carrier lifetimes Figure 3 depicts the data obtained from time-resolved PL measurements (TRPL), done on as-grown and surface passivated disks-in-NW samples as a function of the temperature with a frequency-tripled (λ=260 nm) mode-locked Tsunami Al_2O_3:Ti laser (pulse width 130 fs; repetition rate 80 MHz, λ=405 nm). The decay times were analyzed with the stretched exponential model : $I=I_0 \exp[-(t/\tau)^{\beta}]$ [11], where the stretching parameter β (here, it is 0.78) is a measure of clustering and related effects due to higher In content. The total carrier lifetime (τ) is derived from the fitting. Furthermore, using the equation : $1/\tau = 1/\tau_r + 1/\tau_{nr}$, and $\eta = 1/(1+ \tau_r/\tau_{nr})$, and the IQE obtained from TDPL, radiative (τ_r) and nonradiative (τ_{nr}) carrier lifetimes are calculated for as-grown and surface passivated samples, which are listed in Table 1. The measured radiative lifetimes are significantly smaller than those measured in equivalent quantum wells [12], due to the confinement of carriers in the radial direction and weaker piezoelectric field due to reduced strain in the nanowires. For the as-grown sample (IQE~43%), τ_r is greater than τ_{nr} at room temperature, but opposite is true for parylene passivated samples (IQE~53%). As can be seen in Fig. 3(b) and (c), τ_r remains almost invariant with temperature, whereas τ_{nr} decreases toward room temperature due to the activation of nonradiative centers.

Table 1 Carrier lifetimes of green emitting as-grown and surface passivated samples at T=300 K.

Sample	Passivation	τ_r(ps)	τ_{nr} (ps)	τ (ps)
	as-grown	748	565	322
Green	Si_3N_4	745	743	365
	Parylene	746	840	395

3.3 Diode characteristics Figure 5(a) depicts room temperature current-voltage characteristics of a fabricated LED. The series resistance of the diode was measured to be 24 Ω and the diode exhibits a turn-on voltage of ~5 V. We believe that the large series resistance is due to a non-optimized doping level of the electron blocking layer and perhaps the larger (than necessary) length of the p-GaN contact layer. The light emission area is 7.8×10^{-4} cm^{-2} and the fill factor of the nanowires was estimated to be 35%. The inset of Fig. 5(a) shows an optical micrograph of the device, which shows that the electroluminescence (EL) distribution is homogeneous over the entire device. Room temperature EL measurements were performed on these devices with different injection currents [Fig. 5(b)]. As shown in Fig. 5(c), the peak wavelength exhibits a blueshift (7 nm) when the injected current is increased to 80 mA (current density=293 A/cm^2), beyond which the emission peak remains invariant up to 102 mA (current density = 375 A/cm^2). From the blueshift of peak wavelength, the polarization field is calculated to be 605 kV/cm [13,14], which is much smaller than that of InGaN quantum wells grown on c-plane sapphire substrate (~2 MV/cm) [15] due to the radial strain relaxation during epitaxy.

A plot of the external quantum efficiency (EQE) in arbitrary units as a function of injection current density, derived from the EL measurements, is shown in Fig. 5(d). The electroluminescence was measured under pulsed bias conditions (pulse width = 1 ms, duty cycle = 0.1%) to minimize heating effects. As seen in Fig. 5(d), the EQE of sample B is low compared to sample A due to higher nonradiative recombination rate in sample B through surface states in absence of passivation. No efficiency droop was observed up to a current density of 375 A/cm^2 for sample A. The slow rise in the EQE for nanowire LEDs has been reported in literature [16-18]. The IQE as a function of injection current density was calculated using the relation: $\eta = Bn^2/(An+Bn^2+Cn^3)$, where n is the injected carrier density and A, B, and C are the Shockley–Read–Hall coefficient, the radiative recombination coefficient and the Auger recombination coefficient, respectively. The value of n is obtained from the relation: $J=qd(An+Bn^2+Cn^3)$, with the effective recombination thickness for each disk was taken to be ~2 nm. The calculated variation of IQE with current density, also shown in Fig. 5(d), was obtained with $A=3.96 \times 10^7$ s^{-1}, $B=2.9 \times 10^{-11}$ cm^3 s^{-1}, and $C = 2.85 \times 10^{-34}$ $cm^6 s^{-1}$ for the unpassivated sample B, and

© 2013 WILEY-VCH Verlag GmbH & Co. KGaA, Weinheim

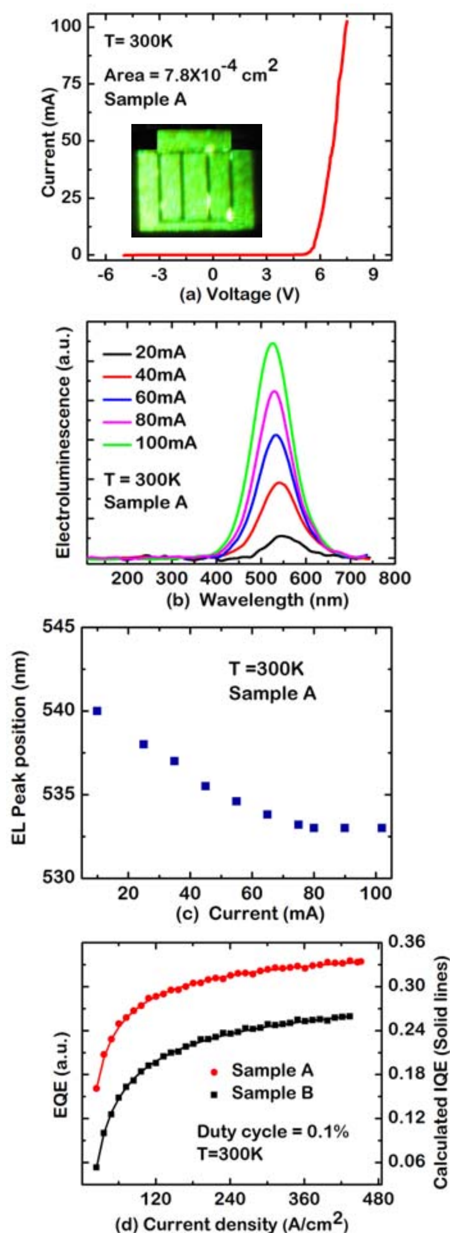

Figure 5 (a) Room temperature I-V characteristics of the fabricated device. The inset shows an optical micrograph of the fabricated LED, (b) room temperature EL of the fabricated device measured under different injection currents, (c) variation in peak wavelength, (d) measured EQE is shown in arbitrary units. Calculated IQE of the LED based on the ABC recombination model is shown by solid line and is in good agreement with measured EQE.

with $A=3.82x10^{7}$ s^{-1}, $B=3.04x10^{-11}$ cm^{3} s^{-1}, and $C=2.71x10^{-34}$ cm^{6} s^{-1} for passivated sample A.

It should be noted that the Auger coefficient C obtained from the analysis has a value ~10^{-34} cm^{6} s^{-1} for both samples A and B. This value agrees with theoretical calculations made for InGaN disks-in-nanowires [19, 20]. It can be seen that there is good agreement between the calculated IQE and measured EQE with variation in current density.

4 Conclusion In conclusion, we have demonstrated the increase in IQE of InGaN disks in GaN nanowires by around 10% through surface passivation. We derived total, radiative and nonradiative carrier lifetimes for green emitting InGaN quantum disks, which are useful for analyzing various green light sources containing these InGaN disks. We have compared the relative EQE of as-grown and surface passivated LEDs, which indicates that surface passivation can enhance electro-optical device performance in terms of light output.

Acknowledgements The work has been supported by the National Science Foundation (MRSEC program) under Grant 0968346.

References

[1] Z. Zhong, F. Qian, D. Wang, and C. M. Lieber, Nano Lett. **3**, 343 (2003).
[2] A. Kikuchi, M. Kawai, M. Tada, and K. Kishino, Jpn. J. Appl. Phys. **43**, L1524 (2004).
[3] W. Guo, A. Banerjee, P. Bhattacharya, and B. S. Ooi, Appl. Phys. Lett. **98**, 193102 (2011).
[4] H. P. T. Nguyen, K. Cui, S. Zhang, S. Fathololoumi, and Z. Mi, Nanotechnol. **22**, 445202 (2011).
[5] Y. P.Varshni, Physica **39**, 149 (1967).
[6] H.P.T. Nguyen, M. Djavid, K. Cui, and Z. Mi, Nanotechnology **23**, 194012 (2012).
[7]L. Wang, M. I. Nathan, T. H. Lim, M. A. Khan, and Q. Chen, Appl. Phys. Lett. **68**, 1267 (1996).
[8] A. C. Schmitz, A. T. Ping, M. A. Khan, Q. Chen, J. W. Yang, and I. Adesida, Semicond. Sci. Technol. **11**, 1464 (1996).
[9] S . Chevtchenko, X . Ni, Q . Fan, A. A. Baski, and H. Morkoc, Appl. Phys. Lett. **88**, 122104 (2006).
[10] W. Guo, A. Banerjee, M. Zhang, and P. Bhattacharya, Appl. Phys. Lett. **98**, 183116 (2011).
[11] I. L. Krestnikov, N. N. Ledentsov, A. Hoffmann, and D. Bimberg et al., Phys. Rev. B **66**, 155310 (2002).
[12] C.Y. Chen, Y. C. Lu, D. M. Yeh, and C. C. Yang, Appl. Phys. Lett. **90**, 183114 (2007).
[13] R. Cingolani, A. Botchkarev, H. Tang, and H. Morkoc, Phys. Rev. B **61**, 2711 (2000).
[14] E. Kuokstis, C. Q. Chen, M. E. Gaevski, W. H. Sun, J. W. Yang, G. Simin, and M. A. Khan, Appl. Phys. Lett. **81**, 4130 (2002).
[15] Y. D. Jho, J. S. Yahng, E. Oh, and D. S. Kim, Phys. Rev. B **66**, 035334 (2002).
[16] H. P. T. Nguyen, K. Cui, S. Zhang, S. Fathololoumi, and Z. Mi, Nanotechnology **22**, 445202 (2011).
[17] H. P. T. Nguyen, S. Zhang, K. Cui, X. Han, et al., Nano Lett. **11**, 1919 (2011).
[18] W. Guo, M. Zhang, P. Bhattacharya, and J. Heo, Nano Lett. **11**, 1434 (2011).
[19] J. Piprek, Semiconductor Optoelectronic Devices: Introduction to Physics and Simulation (Academic Press, San Diego, CA, 2003).
[20] J. Hader, J. V. Moloney, B. Pasenow, S. W. Koch, M. Sabathil et al., Appl. Phys. Lett. **92**, 261103 (2008).

 © 2013 WILEY-VCH Verlag GmbH & Co. KGaA, Weinheim